FRONT SIDE ANTIREFLECTION CONCEPTS FOR SILICON SOLAR CELLS WITH DIFFRACTIVE REAR SIDE STRUCTURES

A.J. Bett[1*], J. Eisenlohr[1], O. Höhn[1], B. Bläsi[1], J. Benick[1], P. Repo[2], H. Savin[2], J.C. Goldschmidt[1], M. Hermle[1]
[1]Fraunhofer Institute for Solar Energy Systems, Heidenhofstr. 2, 79110 Freiburg, Germany
[2]School of Electrical Engineering, Aalto University, 00076 Aalto, Finland
[*]alexander.bett@ise.fraunhofer.de

ABSTRACT: For thin silicon solar cells, standard pyramidal textures cannot be used as antireflection structures due to their thicknesses of several micrometres. In this paper, we investigate two alternative front side antireflection surfaces, which in combination with diffractive rear side structures could lead to low surface reflectance and advanced light trapping: firstly, planar multi-layer antireflection coatings, optimized using experimentally determined refractive indices, have been produced. The resulting hemispheric reflectance weighted with the AM1.5g spectrum (280 nm to 1000 nm) for two and three optimized planar layers were 3.67 % and 3.52 %, respectively, slightly higher than for a sample with inverted pyramids with 3.09 %. Secondly, black silicon was investigated. This acicular nanostructured silicon surface has a very low reflectance over a wide range of the spectrum (weighted reflectance 1.21 %). Reflection and transmission measurements show that a black silicon surface leads to scattering and light trapping. As we see significant absorption for energies below the silicon bandgap for all samples with structured surfaces, possible mechanisms leading to these measurement results were analysed.
Keywords: Light Trapping, Antireflection Coating, High Efficiency, Silicon Solar Cell, Black Silicon

1 INTRODUCTION

For thin silicon solar cells optimized light trapping is essential. Pyramidal textures on the front side and a planar reflector on the rear side are currently widely used. For advanced light trapping diffractive rear side structures, like gratings produced via nano-imprint lithography or self-assembled hexagonal sphere gratings, have been proposed and successfully realized [1-3].

For highest efficiencies, however, the combined performance of front and rear side needs to be investigated. Therefore, in this paper we investigate two different concepts of front side antireflection treatment, which are intended to be used in conjunction with diffractive rear side structures: First optimized planar multi-layer systems, and second black silicon, a nano-structured acicular silicon surface fabricated by deep reactive ion etching. With such structures a very low reflectance over a broad spectral range can be achieved [4-7]. Black silicon can be effectively passivated by atomic layer deposition of Al_2O_3, so it is possible to use it in solar cells [4, 8, 9].

Figure 1 shows a sketch of the light trapping in silicon due to a hexagonal sphere grating [1] on the rear side and a multi-layer planar antireflection coating (a) and black silicon (b), respectively, on the front side.

In section 2 of this paper optimized planar multilayer systems for front side antireflection coating are investigated. In section 3 the low reflectance and scattering effects of black silicon are discussed. In absorption measurements on samples with structured surfaces a parasitic absorptance of photons with energies below the silicon bandgap appears. We investigated possible causes for this effect and present our results in section 4.

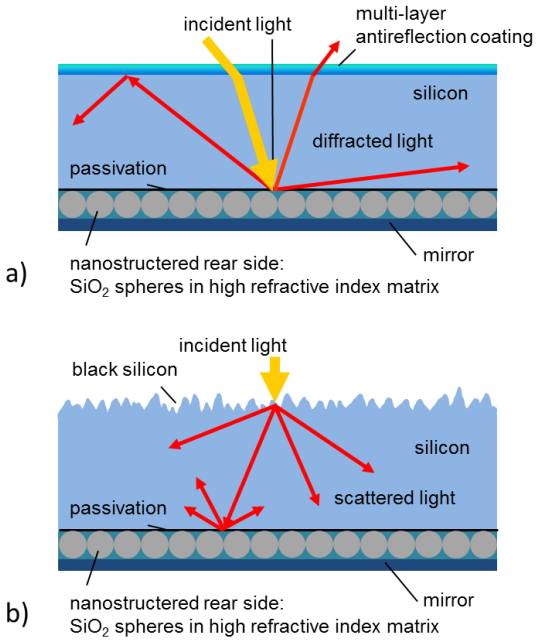

Figure 1: Sketch of a crystalline silicon solar cell with a hexagonal sphere grating on the rear side and a) a multi-layer antireflection coating or b) black silicon on the front side.

2 OPTIMIZED PLANAR MULTILAYER SYSTEMS

Planar multi-layer systems were optimized to serve as two and three layer antireflection coatings. We used a genetic algorithm [10] based on the transfer matrix formalism [11]. The algorithm operates with experimentally determined, wavelength dependent complex refractive indices of several dielectric materials. It varies the materials and the layer thicknesses to find the best combination. The optimization parameter is the transmittance through the antireflection layers into the silicon bulk weighted by the AM1.5g spectrum [12] and the internal quantum efficiency of a highly efficient

silicon solar cell. Optimizations were carried out with air as incident medium and additionally with EVA to consider the situation in a module. In the module case the transmittance from air to EVA through 3 mm of glass and 460 µm of EVA is considered as an additional weighting function. A 10 nm Al_2O_3 passivation layer directly on the silicon bulk is also considered.

In Table I the results of the optimization in the module case are listed. For comparison a system consisting of only one single layer has also been optimized. The multi-layer systems have a higher weighted transmittance than a single layer. The difference between two and three optimized dielectric layers is very small.

Table I: Optimization of planar antireflection coatings for the module case. T_w is the optimization parameter, the weighted transmittance from EVA through the optimized layer system and a 10 nm Al_2O_3 passivation layer to the silicon substrate.

1 layer	2 layers	3 layers
52 nm TiO_2	69 nm SiN_xO_y 58 nm TiO_2	71 nm SiN_xO_y 27 nm TiO_2 22 nm SiC_x
T_w = 94.53 %	T_w = 96.03 %	T_w = 96.48 %

Table II shows the results of the optimization with air as incident medium. Like in a module, systems consisting of two and three layers perform almost equally well, but significantly better than a single layer antireflection coating. The reflectance of these systems has been simulated considering a 250 µm thick silicon wafer using the transfer matrix formalism and the reflectance weighted with the AM1.5g spectrum in the range of 280 nm to 1000 nm R_g has been calculated. In contrast to T_w, where silicon is treated as a half-endless substrate, this value can be compared with measurement data directly.

Table II: Optimization of planar antireflection coatings for air as incident medium. T_w is the optimization parameter, the weighted transmittance through the layer system. R_g is the simulated reflectance weighted by the AM1.5g spectrum in the range of 280 nm to 1000 nm.

1 layer	2 layers	3 layers
82 nm SiN_xO_y	97 nm SiO_2 59 nm TiO_2	94 nm MgF_2 29 nm SiN_xO_y 47 nm TiO_2
T_w = 90.65 % R_g = 8.68 %	T_w = 96.13 % R_g = 3.57 %	T_w = 96.39 % R_g = 3.32 %

The planar multilayer systems listed in Table II have been produced on 250 µm thick silicon wafers. TiO_2 and MgF_2 were deposited by evaporation, SiO_2 and SiN_xO_y by plasma enhanced chemical vapour deposition (PECVD). Figure 2 shows scanning electron microscope pictures of the deposited dielectric layers. The layer thicknesses indicated in the pictures have been measured using spectroscopic ellipsometry. The difference between the measured values and the values presented in Table II is due to process instabilities.

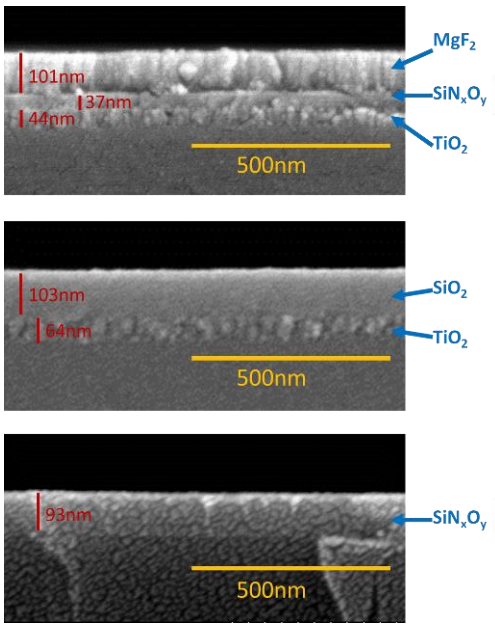

Figure 2: SEM pictures of the fabricated optimized multi-layer systems. The indicated layer thicknesses have been determined by spectroscopic ellipsometry.

For the three produced systems, the reflectance has been measured. The measured reflectance is presented in Figure 3 and compared to the reflectance of an also 250 µm thick sample with inverted pyramids with a single layer antireflection coating consisting of Si_3N_4 deposited by PECVD on the front side.

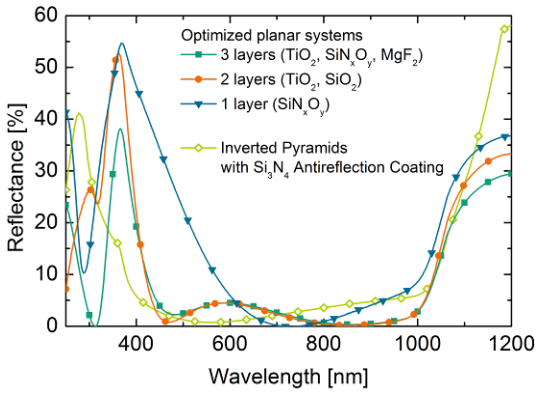

Figure 3: Measured reflectance of the different multilayer systems. For comparison the reflectance of a sample with inverted pyramids coated with Si_3N_4 is displayed.

The reflectance weighted with the AM1.5g spectrum in the range of 280 nm to 1000 nm R_g has been calculated for all curves shown in Figure 3. The value of R_g is 3.52 % for the three layer system and 3.67 % for the two layer system. For the sample with inverted pyramids and an antireflection coating, we determined a weighted reflectance of 3.09 %. Theoretically the value of R_g for such a pyramidal structure should be 2.86 %. With random pyramids an even lower value of 2.09 % could be achieved. The theoretical values have been calculated using the online simulation tool OPAL 2 from PV Lighthouse [13]. In comparison to inverted pyramids the reflectance of the optimized planar systems is still higher, but this reflectance loss might be overcompensated by

electrical gains due to the flat front surface and by an optimized light trapping, when a diffractive rear side structure is realized.

The produced two and three layer systems behave almost as well as expected from the optimization (see Table II). The difference in the weighted reflectance is very low (0.1 % and 0.2 % respectively), although the layer thicknesses between the optimized and realized systems differ significantly as can be seen in Table II compared to Figure 2 due to process variations. For the antireflection coating consisting of only one layer, the difference in the weighted reflectance is much higher (8.68 % in the simulated system and 9.98 % in the realized system). Hence, we can conclude that in addition to the lower reflectance, multi-layer systems are less dependent of process instabilities than a single layer system.

3 BLACK SILICON

As a second alternative front side antireflection - surface, black silicon was investigated. In general, black silicon designates surface nanostructures of variable structure size produced with different techniques. The black silicon considered in this work is fabricated by reactive ion etching. The height of the structure is about 1 µm. Figure 4a shows the measured reflectance of a wafer with black silicon on the front side and a planar rear side. The reflectance in the range of 280 nm to 1000 nm weighted by the AM1.5g spectrum is 1.21 % and therefore almost 2 % lower than in the case of inverted pyramids with an antireflection coating on the front side. In Figure 4b a scanning electron microscope (SEM) picture of the nanostructured surface is shown.

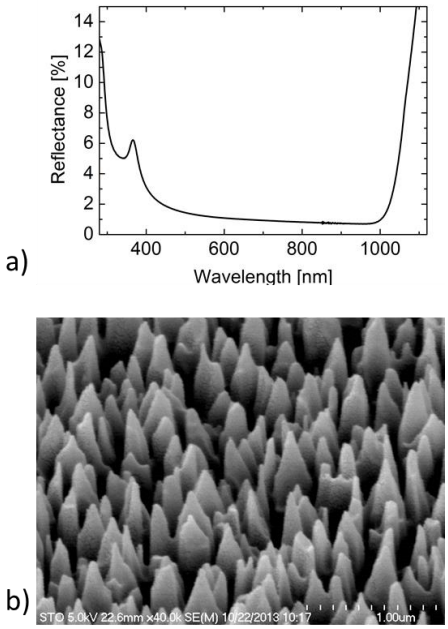

Figure 4: a) Measured reflectance and b) SEM picture of black silicon.

Black silicon not only has a very low reflectance but also leads to light trapping due to scattering effects. To estimate the scattering properties of black silicon reflectance and transmittance measurements have been conducted.

In reflectance measurements the aperture diameter of the integrating sphere in the reflectance measurements of samples with black silicon on the front side and a planar rear side was varied. The reflectance signal decreases with the diameter of the hole in the integrating sphere as shown in Figure 5. This means, that incident light is scattered in the black silicon structure. If the scattering angle is greater than 16°, light will be reflected at the rear side by total internal reflection and redirected towards the front where it will mostly leave the sample. Depending on the aperture diameter, a part of the scattered light cannot re-enter the integrating sphere (see sketch in Figure 6). The illustrated behaviour shows that a significant part of light is scattered at high angles.

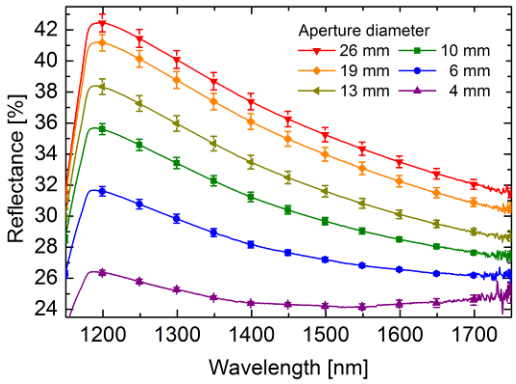

Figure 5: Measured reflectance of samples with black silicon on the front side and a planar rear side for different aperture diameters of the reflection port of the integrating sphere. The measured reflectance signal decreases with decreasing aperture diameter because light scattered at high angles cannot re-enter the sphere and reach the detector.

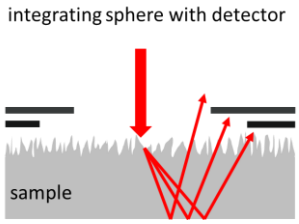

Figure 6: Sketch of reflectance measurement with different aperture diameters. Without aperture, all sketched rays can reach the detector. With decreasing aperture diameter more and more rays cannot re-enter the sphere.

Scattering effects can also be seen in transmittance measurements. For wavelengths above about 1000 nm, where the absorption length in silicon exceeds the wafer thickness of 250 µm, light is partly transmitted through the sample. Light can be transmitted directly passing straight through the wafer or transmitted diffusely when scattered by the textured surface. Figure 7 compares two types of transmittance measurements of samples with black silicon on the front side and a planar rear side: A hemispherical transmittance measurement with an integrating sphere, where all transmitted light is detected, and a direct transmittance measurement without integrating sphere, where only directly transmitted light is detected. The hemispheric transmittance signal is significantly higher than the direct transmittance signal, hence a part of the light is scattered due to the black

silicon surface. Of course, only light scattered in angles less than 16° can be detected in transmittance measurements. For higher angels, total internal reflection prevents light from leaving the sample at the rear side.

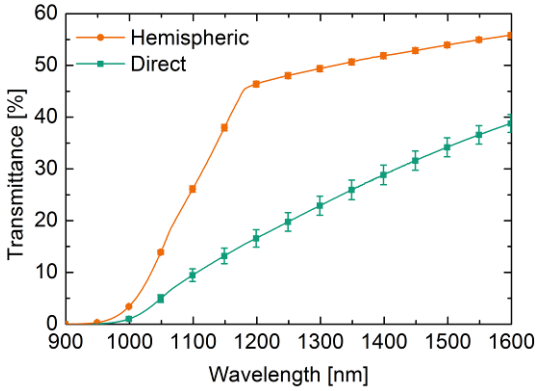

Figure 7: Measured direct and hemispheric transmittance of samples with black silicon on the front side and a planar rear side. The hemispheric transmittance is considerably higher than the direct transmittance. Therefore light must be partly scattered due to the black silicon surface.

The absorptance *A* has been determined for samples with - inverted pyramids with a single antireflection layer consisting of Si_3N_4 and black silicon and planar rear sides from reflectance *R* and transmittance *T* measurements by *A*=1-*T*-*R*. Figure 8 shows that the light trapping properties of these two structures are comparable. For both structures the absorptance in the infrared near the silicon bandgap is obviously better than for a graded index layer, where the complex refractive index is continuously varied from air to silicon so that a perfect antireflection coating can be achieved. However, a graded index layer is planar and cannot lead to diffraction or scattering of light. The absorptance for black silicon samples as well as for samples textured with inverted pyramids is still lower than the Yablonovitch limit for the absorptance of a perfect diffuse scatterer [14]. To further approach the Yablonovitch limit a combination of a front side structure and a diffractive rear side structure will be needed.

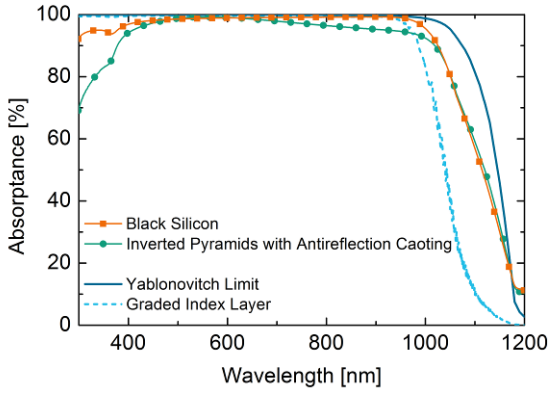

Figure 8: Absorptance of samples with black silicon and inverted pyramids with a single layer antireflection coating respectively on the front side and a planar rear side determined from reflectance and transmittance measurement. The absorptance of a graded index layer and a perfect diffuse scatterer (Yablonovitch limit) has been simulated.

4 NEAR INFRARED ABSORPTION

In all our measurements of structured silicon wafers (black silicon, inverted pyramids, gratings), we observe a significant absorption for energies below the silicon bandgap. This absorption is sometimes ignored or explained with free carrier absorption (FCA) in literature [6, 8].

To explain this parasitic absorption in the near infrared, FCA was initially investigated. Reflectance and transmittance have been measured for five differently doped p-type silicon wafers with inverted pyramids on the front side and a planar rear side. Again, absorptance was calculated via *A*=1-*T*-*R*. Figure 9 shows the measurement results compared to FCA simulations [15].

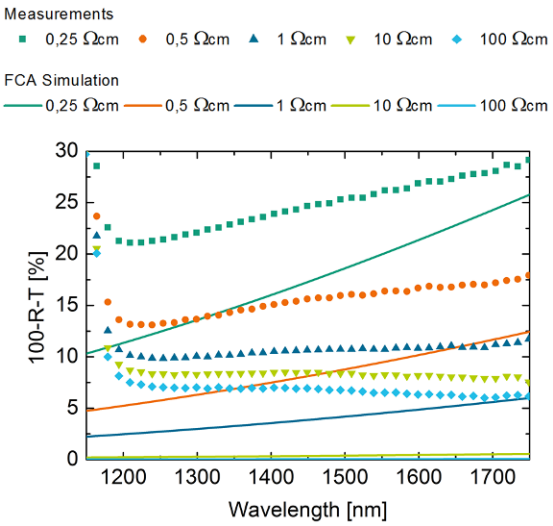

Figure 9: Measured absorptance (symbols) and FCA simulation (lines) for differently doped samples. FCA cannot explain the whole parasitic absorption.

The measured absorptance is considerably higher than the expected FCA. Even for very lowly doped samples (10 Ωcm and 100 Ωcm), where the FCA should be nearly zero, we observe absorptance of about 7 %. Thus, the absorption in the near infrared cannot be

explained completely by FCA.

Based on comparisons with measurements with centre mounted samples, in which also light leaving the sample further away from the excitation spot and at the sample's edges is detected, a small fraction of about 1 % to 3 % absolute can be attributed to light guiding, leaving about 4% un-accounted.

As a further possible explanation for the parasitic absorption surface defects were considered. The samples have been passivated by Al_2O_3 and absorption has been measured again. The results do not show any difference between passivated and unpassivated samples. Absorption from surface defects can therefore not explain the absorption for energies below the silicon bandgap.

5 SUMMARY

Planar multi-layer systems have been optimized with experimentally determined, wavelength dependent complex refractive indices of several dielectric materials to serve as antireflection coatings. The optimized systems have been produced and characterized. There is almost no difference between systems consisting of two or three layers. The reflection weighted with the AM1.5g spectrum in the range of 280 nm to 1000 nm for the deposited systems is 3.67 % in case of two and 3.52 % in case of three layers. These values are only slightly higher than the experimentally observed value of 3.09 % for inverted pyramids with an antireflection coating. This reflectance loss might be overcompensated by electrical gains due to the flat front surface and by an optimized light trapping when a diffractive rear side structure is realized.

For black silicon the reflection weighted with the AM1.5g spectrum in the range of 280 nm to 1000 nm is only 1.21 %. Reflectance and transmittance measurements have shown obvious scattering effects in samples with black silicon on the front side. Absorptance behaviour for wavelengths near the silicon bandgap suggests an equally pronounced light trapping of black silicon samples and samples with inverted pyramids and a single layer antireflection coating. Hence black silicon is a promising alternative front side structure.

Concerning the absorption below the silicon bandgap, there is about 7 % of the absorption remaining that cannot be explained with free carrier absorption. About 1 % to 3 % can be attributed to light guiding. Further investigations are required to explain the parasitic absorption completely.

6 ACKNOWLEDGEMENT

The research leading to these results has received funding from the German Federal Ministry of Education and Research in the project "InfraVolt" (project number 03SF0401B) and from the German Federal Ministry for Economic Affairs and Energy under contract number 0325292 "ForTeS". J. Eisenlohr and O. Höhn gratefully acknowledge the scholarship support from the Deutsche Bundesstiftung Umwelt DBU.

7 REFERENCES

[1] Eisenlohr, J., et al., *Hexagonal sphere gratings for enhanced light trapping in crystalline silicon solar cells.* Optics Express, 2014. **22**(S1): p. A111-A119.

[2] Eisenlohr, J., et al. *Integrating diffractive rear side structures for light trapping into crystalline silicon solar cells*. in *Proceedings of the 28th European Photovoltaic Solar Energy Conference and Exhibition*. 2013. Paris, France.

[3] Mellor, A., et al., *Nanoimprinted diffraction gratings for crystalline silicon solar cells: implementation, characterization and simulation.* Optics Express, 2013. **21**(5): p. A295-A304.

[4] Repo, P., et al., *Effective Passivation of Black Silicon Surfaces by Atomic Layer Deposition.* Photovoltaics, IEEE Journal of, 2013. **3**(1): p. 90-94.

[5] Zilk, M., et al. *RIE Black Silicon for Photovoltaic Application*. in *Renewable Energy and the Environment Congress*. 2013.

[6] Kroll, M., et al. *Black silicon for solar cell applications*. 2012.

[7] Branz, H.M., et al., *Nanostructured black silicon and the optical reflectance of graded-density surfaces.* Applied Physics Letters, 2009. **94**(23).

[8] Otto, M., et al. *Opto-electronic properties of different black silicon structures passivated by thermal ALD deposited Al2O3*. in *Renewable Energy and the Environment*. 2013. Tucson, Arizona: Optical Society of America.

[9] Otto, M., et al., *Extremely low surface recombination velocities in black silicon passivated by atomic layer deposition.* Applied Physics Letters, 2012. **100**(19): p. -.

[10] Höhn, O., et al. *Optimization of angularly selective photonic filters for concentrator photovoltaic*. 2012.

[11] Macleod, H.A., *Thin film optical filters*. 3rd ed. 2001: Taylor & Francis. 668.

[12] IEC, *Photovoltaic devices - part 3: measurement principles for terrestrial photovoltaic (PV) solar devices with reference spectral irradiance data*. . 2nd ed. International Standard, IEC 60904–3. 2008: International Electrotechnical Commission.

[13] *PV Lighthouse OPAL 2 Calculator*. [cited 2014 27.08.]; Available from: http://www.pvlighthouse.com.au/calculators/OPAL%202/OPAL%202.aspx.

[14] Yablonovitch, E., *Statistical ray optics.* Journal of the Optical Society of America, 1982. **72**(7): p. 899-907.

[15] Rudiger, M., et al., *Parameterization of Free Carrier Absorption in Highly Doped Silicon for Solar Cells.* Electron Devices, IEEE Transactions on, 2013. **60**(7): p. 2156-2163.